

COMBINED MODE I-MODE II FRACTURE OF CERAMICS

G. Nicoletto* and L. Esposito‡

The mixed mode fracture behavior of alumina and silicon nitride has been determined with a technique consisting of a pre cracking phase by the BI technique and a fracture testing phase by the asymmetric four point bending configuration. Combined Mode I-Mode II fracture envelopes have been obtained along with the dependence of the initiation angle from the mixed mode loading conditions. The results have been correlated with theoretical predictions and previous data.

INTRODUCTION

The fracture response of ceramics has been mainly characterized under Mode I loading condition although initiation sites of structural failure are often crack-like defects which are arbitrarily oriented with respect to the loading system. While many multiaxial fracture theories have been proposed in the past, an assessment of their applicability to ceramic materials has been lagging since mixed mode fracture data in the literature are scarce and often show large discrepancies, (1-5). Since various testing methods have been proposed, the conflicting results have been attributed either to unreliable experimental procedures or to a critical interaction of material and test method.

This paper is aimed at presenting original combined Mode I/Mode II fracture data obtained on two ceramics. To discuss the relevance of the present results, two aspects will receive special attention: a) the pre cracking technique which is known to be critical for this class of materials; b) the specimen geometry-material interaction.

* Industrial Engineering Dept., University of Parma, Italy

‡ Italian Ceramic Center, Bologna, Italy

As far as point a), the authors have been extensively using the bridge-indentation pre cracking technique, (4). In this way reproducible natural pre cracks have been routinely inserted in bars to be subsequently tested in mixed mode according to the asymmetric four point bending scheme. To deal with point b), mixed Mode I-Mode II fracture envelopes have then been obtained with different materials while keeping specimen geometry and pre crack type and size constant. The results are also used in an analysis of mixed mode fracture theories and correlated with literature data obtained with different specimen geometries.

EXPERIMENTAL DETAILS

Materials

The ceramics investigated in this study were: two batches of a commercial alumina (Degussit AL23) and a silicon nitride (Morgan-Matroc AME RBSN). The alumina was 99.6 pure (in wpc.) with a Young's modulus $E = 350$ GPa, a nominal compressive strength $\sigma_c = 600$ MPa and an average grain size $d = 10$ μm . The bending strength of the two batches, from now on denoted with letter A and C, respectively, were determined on several prismatic bars failed under four-point bending σ_F (A) = 214 MPa and σ_F (C) = 167 MPa. The micro structure was characterized by thermal etching and an automatic video analysis was carried out to identify morphological differences. The reaction-bonded Si_3N_4 , had a Young's modulus $E = 170$ GPa, a nominal compressive strength $\sigma_c = 650$ MPa and a bending strength $\sigma_F = 200$ MPa. The micro structure was rather inhomogeneous and characterized by 20% open porosity.

Mixed mode fracture testing method

The mixed mode fracture testing method used in this work, (4), consisted of : i) the introduction of a natural pre crack in a prismatic bar according to the bridge indentation BI technique, (6), and ii) the fracture test of the bar under controlled asymmetric four-point bending loading. The BI pre cracking technique involves a preliminary Vickers indentation performed on the surface of the bar to induce a system of micro cracks, (4). The specimen is then inserted in a loading device schematically depicted in Figure 1 with the indentation straddling the lower gap. A compressive loading is gradually applied to the specimen up to the level at which the indentation crack is observed to pop-in to a through-the-thickness configuration according to the scheme of Figure 1. A thorough characterization of the pre cracking parameters is reported elsewhere, (4). The specimen containing the through-the-thickness pre crack is then fractured using the asymmetric four-point bending configuration of Figure 2 in which various ratios of shear force vs. bending moment can be imposed on the specimen by controlling the offset distance S of the

pre crack from the anti symmetry axis. The shear force and the bending moment acting on the plane of the pre crack result in a combined Mode I / Mode II loading at the crack tip . A pure Mode II condition is obtained when $S = 0$. Pure Mode I fracture toughness is determined using the classical symmetrical four-point-bending configuration.

For given offset S , pre crack length a and fracture load P applied by the testing machine, the mixed mode fracture toughness are determined with the following equations

$$K_I = F_I \left(\frac{a}{W} \right) \frac{6M}{tW^2} \sqrt{\pi a} \quad (1)$$

$$K_{II} = F_{II} \left(\frac{a}{W} \right) \frac{V}{tW} \sqrt{\pi a} \quad (2)$$

where $M=PcS(b-c)/(b+c)$ and $V=Pc(b-c)/(b+c)$, t and W are thickness and width of the bar, respectively, b and c are defined in Figure 2 and $F_I(a/W)$ and $F_{II}(a/W)$ are geometry factors discussed elsewhere, (4). After fracture testing, specimen halves have been examined in the optical microscope to measure the angle formed between the pre crack and the initial stage of the mixed-mode propagation.

RESULTS AND DISCUSSION

Mixed mode fracture behavior

The pure Mode I fracture toughness, K_{IC} , of the various materials was initially determined. The alumina showed quite a significant batch-to-batch variation, in fact $K_{IC} (A) = 3.91 \pm 0.13 \text{ MPa(m)}^{1/2}$, and $K_{IC} (C) = 5.46 \pm 0.14 \text{ MPa(m)}^{1/2}$ (i.e. the second number is the standard deviation). These values in themselves are reasonable when compared with the literature, although an over 30% increase in toughness for nominally the same material is surprisingly large: the two batches, however, were already found to significantly differ in bending strength (20% difference). The silicon nitride, on the other hand, showed a $K_{IC} = 2.91 \pm 0.07 \text{ MPa(m)}^{1/2}$ which is in line with reported values.

The pure Mode II fracture toughness was subsequently obtained using the four-point asymmetric testing configuration (i.e. $S = 0$ in Figure 2). The alumina of the first batch showed $K_{IIC} (A) = 3.75 \pm 0.07 \text{ MPa(m)}^{1/2}$ while the second batch yielded $K_{IIC} (C) = 3.32 \pm 0.15 \text{ MPa(m)}^{1/2}$. These results do not confirm the large batch-to-batch difference found during Mode I testing and show a scatter comparable also to Mode I testing. This observation allows an assessment of the experimental

procedure which is significantly more complex than the Mode I version because it involves an accurate positioning of the pre crack. In the silicon nitride $K_{IIc} = 3.21 \text{ MPa(m)}^{1/2}$ again with limited scatter.

By varying S shown in Figure 2 combined Mode I - Mode II loading conditions were investigated. Mixed mode fracture toughnesses, K_I and K_{II} , are displayed in the single plot of Figure 3 where the mixed mode envelope of the materials can be readily identified. The two batches of alumina show a regular response in dependence to the degree of loading mixity. The silicon nitride, on the other hand, reveals a discontinuity in the envelope: a small contribution of Mode II loading results in a significant drop in toughness which is not confirmed with further increase in the Mode II component. This peculiar effect is presented because repeated tests confirmed the response and, although no explanation is offered at the moment, a possible source could be related to a crack interaction with the relevant percentage of material porosity.

In the experiments care was devoted to the measurement of the angle formed between the crack initiation direction under mixed mode conditions and the pre crack direction. Data obtained in this study on alumina and silicon nitride are summarized in Figure 4 along with data on similar materials from the literature, (5). They show limited material dependence of the fracture initiation angle.

Correlation with mixed mode fracture theories

To assess and hopefully generalize the present results, a correlation with theoretical modeling of the mixed mode fracture behavior of solids is attempted. Although a presentation of the fracture theories proposed in the past is beyond the scope of this paper, it is pointed out that the mixed mode fracture response of brittle materials has been discussed referring to three main hypotheses: i) the maximum hoop stress theory, (7); ii) the minimum strain energy density theory, (8); iii) the strain energy release rate theory, (9).

The fracture theories usually predict the Mode II fracture toughness on the basis of the sole Mode I fracture toughness. The theoretical K_{IIc}/K_{Ic} ratios range between 0.63 and 1.1 with the most cited values of 0.866 for the maximum hoop stress theory and 1.02 for the minimum strain energy density theory ($\nu = 0.25$). In the present experiments the K_{IIc}/K_{Ic} ratio is 0.96 for the alumina A and 0.61 for alumina C while for the silicon nitride $K_{IIc}/K_{Ic} = 1.10$. In general, all the values fall within the range of the theoretical predictions and two out of three data support the minimum strain energy density theory. The value found in the alumina A agrees with data obtained with bend bars and fatigue pre cracks, (3). Recent data on alumina and silicon nitride determined with an analogous testing technique, (5), also indicated a good correlation with the same theory. Alumina C shows a considerably

lower value although in the literature K_{IIc}/K_{IC} values ranging from 0.6 to 2.0 are reported, (1-5). In Figure 5 fracture envelope predicted by the minimum strain energy density theory for $\nu = 0.25$ is plotted along with the normalized experimental data of Figure 3. When the three materials are considered simultaneously the scatter is significant even though each single material is reasonably well-behaved.

Most fracture theories also predict the initiation angle formed by the direction of propagation and the pre crack, in particular, when a pure Mode II condition is applied: it is found to vary in a narrow range from 70 to 80 degrees. In the light of these predictions the data of Figure 4 for a mode mixity ratio $K_{II}/(K_I+K_{II}) = 1$ show experimental angles which are considerably smaller. The trend of the experimental data on two materials, although common to data of (5), is always below the theory. Since the present authors as well as other researchers found a good correlation with the theoretical angles when testing other materials, namely glass, (4), and PMMA, it appears that the response of Figure 4 is peculiar of the ceramic materials and apparently tells that in these materials crack initiation is controlled by the far-field tensile stress rather than the crack tip stress fields.

Influence of testing technique on mixed-mode fracture behavior

The experimental evidence collected in the recent years points out that the response of ceramic materials to mixed mode loading is affected by factors such as the type of pre crack and the specimen geometry. The insertion of a crack-like feature in a ceramic specimen is a major difficulty which has been attacked using machined slots, (1), chevron notches, (2), pre cracks grown out of notches in compression fatigue, (3), and recently BI pre cracks, (4,5). Different fracture specimen geometries have been used to test ceramics in mixed mode: tubes in torsion, (1), disks in compression, (2), and bend bars, (3-5). In Figure 6 a summary of experimental evidence collected with the present technique in three materials, namely glass, (4), alumina and silicon nitride, is presented adopting the compact representation given by the parabolic function often assumed to represent the mixed mode fracture envelope after suitable normalization, (9),

$$\frac{K_I}{K_{IC}} + \left(\frac{K_{IC}}{K_{IIc}} \right)^2 \left(\frac{K_{II}}{K_{IC}} \right)^2 = 1 \quad (4)$$

Literature data for the same materials obtained with different techniques are also introduced in Figure 6 to show by comparison the effect of the testing technique. In Figure 6 AB indicates the present technique, given by a combination of BI and asymmetric bending of a prismatic bar, CD relates to the use of the chevron-notched disk in compression, (2), TP refers to the tensile panel with an inclined crack and TT torsion loading of a slotted tube, (1). Figure 7 shows that the

TP and TT techniques determined the lowest K_{II} response and the CD technique yields always the highest K_{II} resistance while the present technique in the various materials shows an intermediate response.

The high Mode II fracture strength determined by the CD technique has been explained, (2,3), in terms of friction conditions between the two planes of the pre crack. Resistance to the sliding motion is enhanced by the strong compressive component which characterizes this specimen geometry and this effect increases with crack length. According to this mechanism micro structure also plays a role: the different response of glass and alumina of Figure 6 is explained in terms of the micro structure-induced surface roughness in alumina which results in a higher resistance to sliding than the flat surface of the amorphous glass. The TP and TT methods, on the other hand, propagate crack under essentially far-field tensile loading, therefore crack faces interlocking mechanisms are prevented. The present technique, AB in Figure 6, is characterized by 1 to 2 mm-long pre cracks and a combination of bending and shear loading of the crack faces. Therefore, the loading conditions could activate the previous mechanism although to a lower degree than in the CD technique. The micro structural effects could also be present, since the Mode II fracture resistance of glass is lower than in ceramic materials.

These comments have attempted to put in perspective the various mixed-mode fracture testing techniques while neglecting the inevitable scatter associated to the material itself. It is felt that the advantages of the technique used in this work which is characterized by natural cracks of controlled length readily inserted in bend bars which, on the other hand, are easy and inexpensive to prepare and to test and require little material render it competitive for widespread use in the future.

CONCLUSIONS

The mixed mode fracture behavior of alumina and silicon nitride has been determined with a technique consisting of a pre cracking phase by the BI technique and a fracture testing phase by the asymmetric four point bending configuration. Combined Mode I-Mode II fracture envelopes have then been obtained and batch-to batch variation in alumina was identified. Correlation with fracture theories showed that the minimum strain energy density theory describes the behavior of two out of three materials. On the other hand, no correlation between experimental and theoretical initiation angles was found. The testing technique appears to play a role in the mixed-mode fracture behavior of ceramic materials.

ACKNOWLEDGMENT

G.N. gratefully acknowledges M.U.R.S.T. for partial support with 40% funds.

REFERENCES

- (1) Petrovic, J.J., J. Am. Ceram. Soc., vol. 68, no. 6, 1985, pp. 348-55
- (2) Singh, D. and Shetty, D.K., J. Am. Ceram. Soc., 72, 1989, pp. 78-84
- (3) Suresh, S., et al., J. Am. Ceram. Soc., Vol. 73, 1990, pp. 1257-67
- (4) Nicoletto, G., et al., L., Ceramica Acta, Vol.5, 1993, pp. 59-71
- (5) Tikare, V. and Choi, S.R., J. Am. Ceram. Soc., 76, 1993, pp. 2265-72
- (6) Nose, T. and Fuji, T., J. Am. Ceram. Soc., vol. 71, 5, 1988, pp. 328-33
- (7) Erdogan, F. and Sih, G.C., ASME J. Basic Engng., Vol.85, 1963, pp.519-525
- (8) Sih, G.C., Int. J. of Fracture, Vol.10, 1974, pp.305-321
- (9) Palaniswamy, K. and Knauss, W.G., Mechanics Today, 1978, pp. 87-148.

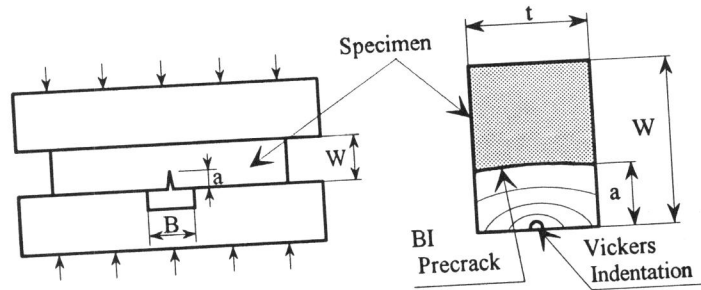


Figure 1 Pre cracking by the bridge indentation technique

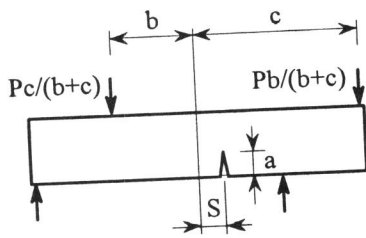


Figure 2 Asymmetrical four-point bending loading

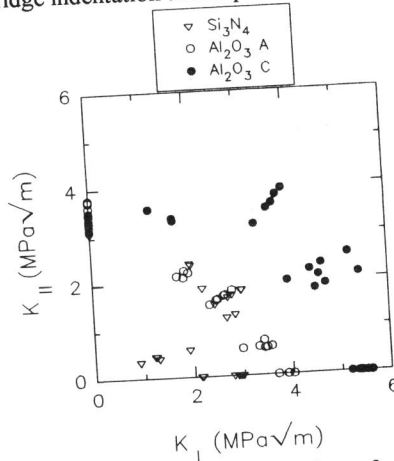


Figure 3 Mixed mode fracture data of alumina and silicon nitride

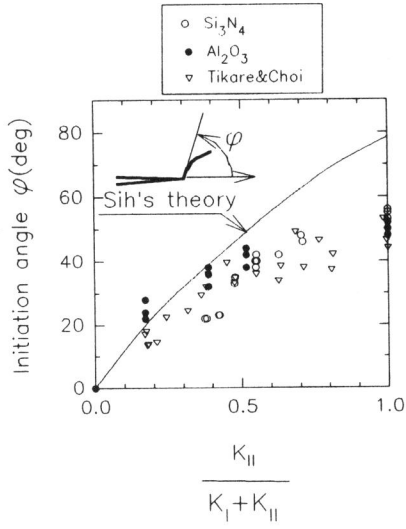


Figure 4 Crack initiation angle as a function of a mode mixity parameter

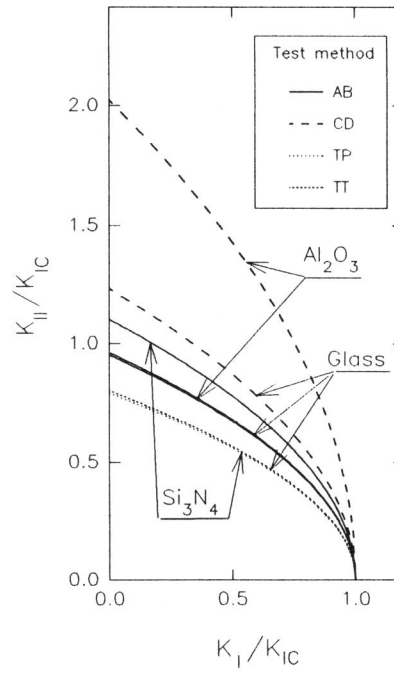


Figure 6 Influence of testing technique and material on mixed mode fracture response

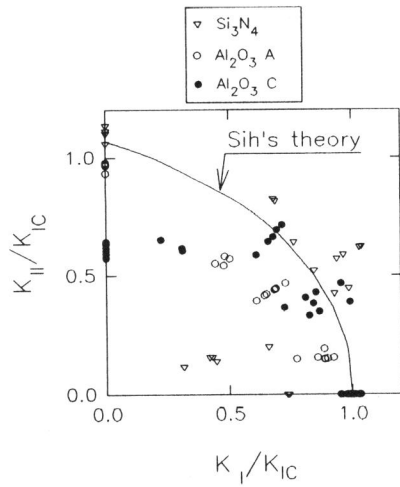


Figure 5 Normalized mixed mode fracture envelopes